Feedback Control of Flow Field behind a Square Cylinder with Inline Oscillations

Sushanta Dutta[1], Krishnamurthy Muralidhar[2], Pradipta K. Panigrahi[2]
[1]Department of Mechanical & Industrial Engineering, IIT Roorkee, Roorkee, India
[2]Department of Mechanical Engineering, IIT Kanpur, Kanpur, India
duttafme.iitr@gmail.com, kmurli@iitk.ac.in, panig@iitk.ac.in

***Abstract*—Control of vortex shedding from a bluff body and vortex induced vibration is of fundamental interest. In recent years a significant amount of work is going on in different engineering and industrial problem such as offshore exploration, marine hydraulics, MEMS (microelectromechanical systems), electronics cooling etc. The present study reports images and signals recorded in the wake of a square cylinder oscillating in the streamwise direction using PIV and HWA. Wakes of a stationary cylinder, one with forced oscillations at the vortex shedding frequency of a stationary cylinder and the flow field resulting from feedback are compared. In the third experiment, cylinder movement is driven by a hotwire signal with the probe placed in the near wake and, in this respect the wake unsteadiness is fed back to the cylinder motion. The amplitude of cylinder movement is about 13% of the cylinder edge. The interest here is towards active control of the flow field at intermediate Reynolds numbers. Experiments have been conducted at Reynolds numbers of 175 and 355. The feedback loop consists of the hotwire probe, phase shifter available in LabVIEW, a power amplifier and electromagnetic actuators. In the presence of cylinder movement, the instantaneous flow field shows suppression of vortex shedding and reduction in velocity fluctuations. The time averaged flow field shows a reduction in the size of the recirculation region with both forced oscillations and feedback when compared to flow past a stationary cylinder. The drag coefficient of a cylinder with forced oscillations is 8% lower than the stationary, while, with feedback, the reduction is 5%.**

Keywords—Wake, Square cylinder, Inline oscillations, Feedback, Particle image velocimetry, Hotwire anemometer.

NOMENCLATURE

f = forcing frequency, Hz

U= upstream velocity, m/s

B= edge of the square cylinder, m

CD= drag coefficient based on the average upstream velocity and edge B.

Re= Reynolds number based on cylinder diameter, $\rho UB/\mu$

rms = root mean square velocity, m/s

u= x-component of velocity, m/s

v= y-component of velocity, m/s

μ= dynamic viscosity, kg/s m2

ρ= density, kg/m3

ωz= spanwise component of the vorticity scaled by U/B

I. INTRODUCTION

Control of bluff body wakes is of fundamental interest as well as practical significance. Flow control can be employed to reduce the intensity of the wake in order to eliminate flow induced oscillation and reduce drag experienced by the object. A variety of control techniques have been proposed. These are classified as active and passive control strategies. In passive control, the flow geometry is altered (Dutta et al., 2008) and there is no external addition of energy. In active control, momentum is transferred over a portion of the boundary to the fluid. Active control can be classified as open and closed loop. A closed loop active control system uses actuators driven by external energy sources through a feedback signal collected from the flow field.

The choice of the transfer function connecting the velocity/pressure signal and the one driving the actuator is crucial for the effectiveness of a feedback signal. For objects that are transversely set in motion by the unsteady forces, literature shows that a control system will best perform when a combination of flow field information and body motion is used for control. Zhang et al. (2003, 2004, and 2005) studied the control mechanism of vortex shedding for a spring loaded square cylinder in cross-flow, whose top surface was perturbed using a piezo actuator. Both closed loop and open loop studies showed a reduction in the time-averaged drag coefficient. The study revealed that closed loop control was more advantageous when compared to the open loop system. Roussopoulos (1993) studied feed back control of vortex shedding for flow past a circular cylinder at an intermediate Reynolds number using flow visualization and hotwire techniques. A loudspeaker was used as an actuator and the hotwire sensor as control. Tau et al (1996) reported a fascinating feedback experiment with a hotwire probe wherein flow visualization was conducted using dye injection technique for flow past a circular cylinder. The flow visualization images clearly showed complete vortex suppression and enhancement for various feedback conditions. Pastoor et al. (2008) studied feedback control of flow over a D-shaped bluff body for drag reduction using experimental and theoretical tools. The derived feedback controller desynchronized the shear-layer, thus postponing vortex formation. The authors achieved 15% drag reduction over a wide range of Reynolds number (23000-70000). Choi et al. (2008) have reviewed recent developments in control techniques for flow over a bluff body. Controls methods are classified in three broad categories: (a) passive and active (b) 2D versus 3D forcing and (c) boundary layer control versus

direct wake modification. Recommendations of various authors have been summarized.

Flow past a square cylinder that is oscillated in the same direction as the incoming flow is discussed in the present work. The flow field is imaged using PIV whereas point measurements have been carried out using hotwire anemometry. The flow field is characterized in terms of time averaged as well as instantaneous quantities such as velocity vectors, rms velocity, vorticity contours, and recovery of the centreline velocity. The time-averaged velocity vectors are used to determine the drag coefficient acting on the cylinder. Wakes of a stationary cylinder, one with forced oscillations at the vortex shedding frequency of a stationary cylinder and the flow field resulting from feedback are compared. As discussed in the previous work of the authors (Dutta et al., 2008), the amplitude and frequency parameters constitute a small perturbation to the wake. The goal of the study is to explore conditions under which the cylinder experiences lower drag and its correlation to the vorticity field.

II. EXPERIMENTAL DETAILS AND THE CONTROL SCHEME

Experiments have been carried out in a low speed vertical test cell made of Plexiglas with air as the working medium. The test cell has two optical windows, one for the passage for laser sheet and other for the recording camera. The cross section of the test cell is 9.5 × 4.8 cm2 and the overall length is 0.4 m. A contraction ratio of 10:1 ahead of the test section has been used. The cylinder (3 × 3 mm2) is square in cross-section and is mounted horizontally with its axis perpendicular to the flow direction. Streamwise oscillations of the cylinder, namely, in a direction parallel to the incoming flow are sustained by electromagnetic actuators. A single wire hotwire anemometer is used to detect wake unsteadiness. The anemometer output voltage was collected in a PC through a data acquisition card (National Instruments) with LABview software. The experimental set-up of the present work and the procedure for PIV measurement are reported by the authors elsewhere (Dutta et al., 2007-2008).

Feedback experiments were conducted in the following manner. A hotwire probe was placed at x/d =5 downstream and y/d=1.2 from the cylinder centre. A long hotwire signal (60000 points) sampled at 1000 values per second was collected in the near wake of a stationary cylinder. This data was subsequently used for generating the feedback signal. The vortex shedding frequency being around 30 Hz, the voltage signal was low-passed filtered at a cut off frequency of 100 Hz to remove the high frequency component. The signal was amplified to the level acceptable to the actuator. A phase shift was given to the filtered signal before sending it to the actuator. By placing the time series of the filtered and amplified signal in a programming loop, it was possible to run the experiment for a long period of time. The schematic layout of the feedback circuit is shown in Figure 1. Results discussed below are for a phase shift of 180o. The largest cylinder displacement within an oscillation is maintained practically constant (at 0.4 mm) in the oscillation experiments with and without feedback. Time traces of the streamwise velocity component in the wake of the cylinder under stationary, forced, and feedback conditions are shown in Figure 2. With feedback, rms velocity fluctuations are seen to be substantially reduced. Further, the spectral characteristics of the signal are also seen to be affected.

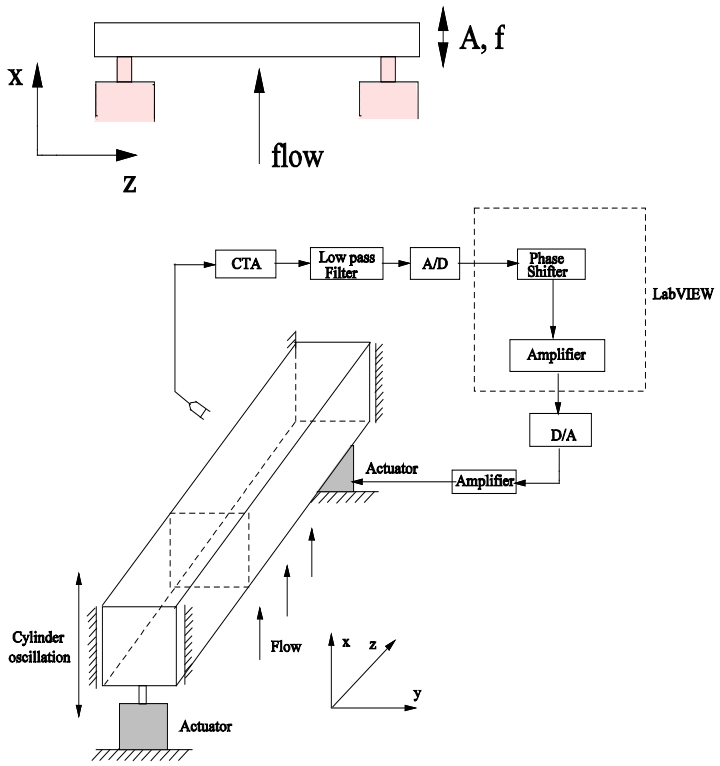

Figure 1 Schematic diagram of the feedback circuit and cylinder oscillation.

III. UNCERTAINTY AND VALIDATION

The seeding of flow with oil particles, calibration, laser light reflection and variation in background illumination, image digitization, calculation of cross correlation, velocity gradients, and out-of-plane particle motion affect the repeatability of PIV measurements. Tracer particles need to follow the main airflow without any lag. For the particle size utilized and the range of frequencies in the wake, a slip velocity error of 0.3–0.5% relative to the instantaneous local velocity is expected. A second source of error in velocity measurement is due to the weight of the particle. In the present experiments, the effect of particle weight was examined by conducting experiments at a fixed Reynolds number by varying the size of the cylinder and air speed. The streamline plot and the dimensionless size of the recirculation region were found to be identical in each case, independent of the fluid speed. Noise due to background light was minimized by using a band pass filter (around the wavelength of the laser) before the camera sensor. The x- and y-component velocity profiles from PIV measurements compared very well to those from the hotwire in the far field region, confirming the proper implementation of both the techniques. From repeated measurements (with Reynolds number kept constant to within ±1%), the uncertainty in drag coefficient was determined to be within ±4% while that in Strouhal number was ±2%. Additional validation of the apparatus is discussed in the previous work of the authors (Dutta et al. 2007, 2008).

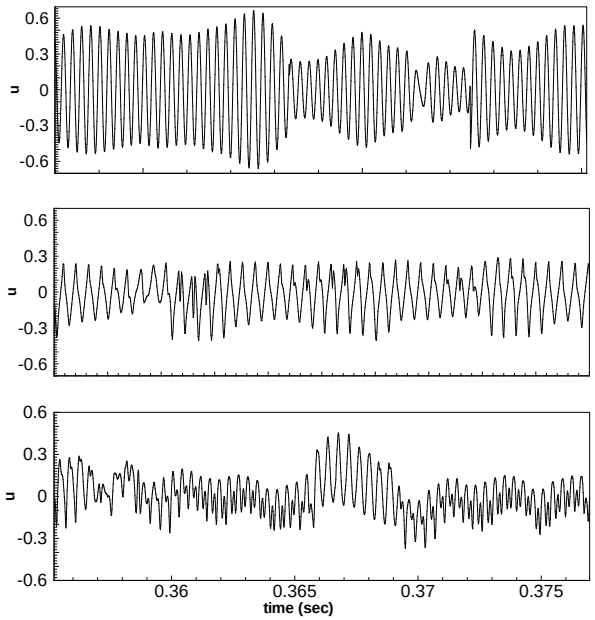

Figure 2 Typical time histories of the streamwise velocity component for a stationary cylinder (upper trace), oscillating cylinder (middle) and oscillating cylinder with feedback (lower trace) at Re=175.

IV. RESULTS AND DISCUSSIONS

Flow patterns are presented in terms of the time-averaged and instantaneous quantities recorded from experiments. Wake dynamics of stationary and oscillating cylinders including the lock-on phenomenon have been discussed by the authors elsewhere (Dutta et al. 2007). The present study aims at examining changes resulting from providing a feedback signal to the actuator. The experiment with open loop (forced) control discussed in the following sections refers to a cylinder oscillated at the frequency of vortex shedding of a stationary cylinder. In the feedback experiments, measurements were carried out with phase angles varying from 0 to 180 degrees. However, the greatest departure from forced oscillations was seen only at a phase angle of 180 degrees. Hence, other experiments are not discussed.

A. Drag Coefficient

Table 1 presents drag coefficients for stationary and oscillating cylinders with and without feedback. Drag coefficient reported here arises from the combined effect of momentum deficit and time-averaged turbulent stresses at the outflow plane of the wake. It has been determined as a time-averaged quantity from a PIV data set of 200 images. The time-averaged drag coefficient has been determined from the profiles of time-averaged velocity profiles and rms velocity fluctuations across the entire test cell at a streamwise location of x/B=10. Drag coefficient is calculated from the extended formula (Lu and Bragg, 2002)

The first term is the momentum deficit of the time-averaged flow field and the second term is the time-averaged contribution of the turbulent fluctuations. In the experiments considered, the second term was found to be 10-15 % of the total drag. The right hand side of Equation 1 yields a momentum loss coefficient. To a first approximation, it is being equated to the drag coefficient. Apart from stationary objects, it is expected to hold for cylinders that are oscillated about a mean position with small amplitude and a frequency close the shedding frequency of a fixed cylinder.

$$C_D = 2\int_{-\infty}^{\infty} \frac{u}{U}\left(1-\frac{u}{U}\right)dy + 2\int_{-\infty}^{\infty} \left(\frac{\overline{v'^2}-\overline{u'^2}}{U^2}\right)dy \quad (1)$$

Table 1 shows that oscillations reduce the drag coefficient with respect to that of stationary cylinder, the reduction being 8% for forced oscillations without feedback and 5% with feedback. These values may be taken to correspond to phase lags of 0 and 180 degrees introduced in the feedback loop. The corresponding wake images are discussed in the following sections.

Table I Drag coefficient (C_D) value for Stationary and Oscillating Cylinder (open loop and closed loop) at Re=175.

Cylinder motion	Stationary	Forced oscillations	With feedback
Drag coefficient (C_D)	1.42 ±3%	1.31 ±4%	1.35 ±4%

B. Velocity Field

Figure 3 shows the time-averaged velocity vectors for stationary and oscillating cylinders, with and without feedback. The grey-scale refers to the velocity magnitude, being dark for zero and bright for the highest value. Figure 3 shows that the near wake velocity is strongly affected by cylinder motion. The size of the velocity deficit zone (in black) reduces in the presence of cylinder oscillation. The recirculation zone is quite small for the open loop system. With feedback, the size of the recirculation zone increases when compared to open loop oscillation. The size of the recirculation zone is related to base pressure and hence related to drag coefficient. Thus, for the choice of parameters, feedback does not appear to have a beneficial effect in diminishing the time-averaged drag coefficient beyond the value for forced oscillations. Zhang et al. (2004) have arrived at a similar conclusion. The proper choice of the feedback parameters is thus, crucial.

C. Vorticity Field and Streamlines

Figure 4(a) shows streamlines in the wake for the stationary, open loop and the feedback oscillation experiments. Streamlines have been derived from the time-averaged velocity vectors recorded by PIV on the plane of the light sheet. The streamline pattern shows that the size of the recirculation bubble reduces for both open loop and feedback experiments. This trend is also visible in the vorticity contours (Figure 4(b)). The recirculation length for feedback control is slightly higher when compared to the open loop. The reduction in vortex formation length indicates directly an increase in the base pressure and hence a reduction in the drag coefficient.

Figure 4(b) compares the time-averaged dimensionless spanwise (ωz) vorticity contours for a stationary cylinder against open loop and feedback controlled oscillations. For the open loop, the vortices move closer to the cylinder and the

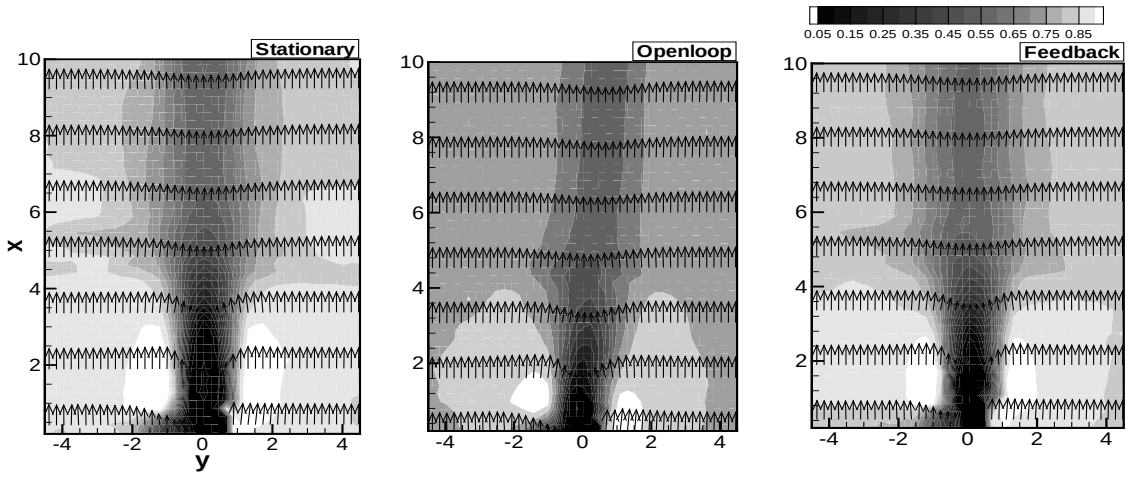

Figure 3 Time-averaged velocity vectors for stationary and oscillating cylinders (with and without feedback) at Re=175. The flooded contours represent the magnitude of the absolute velocity.

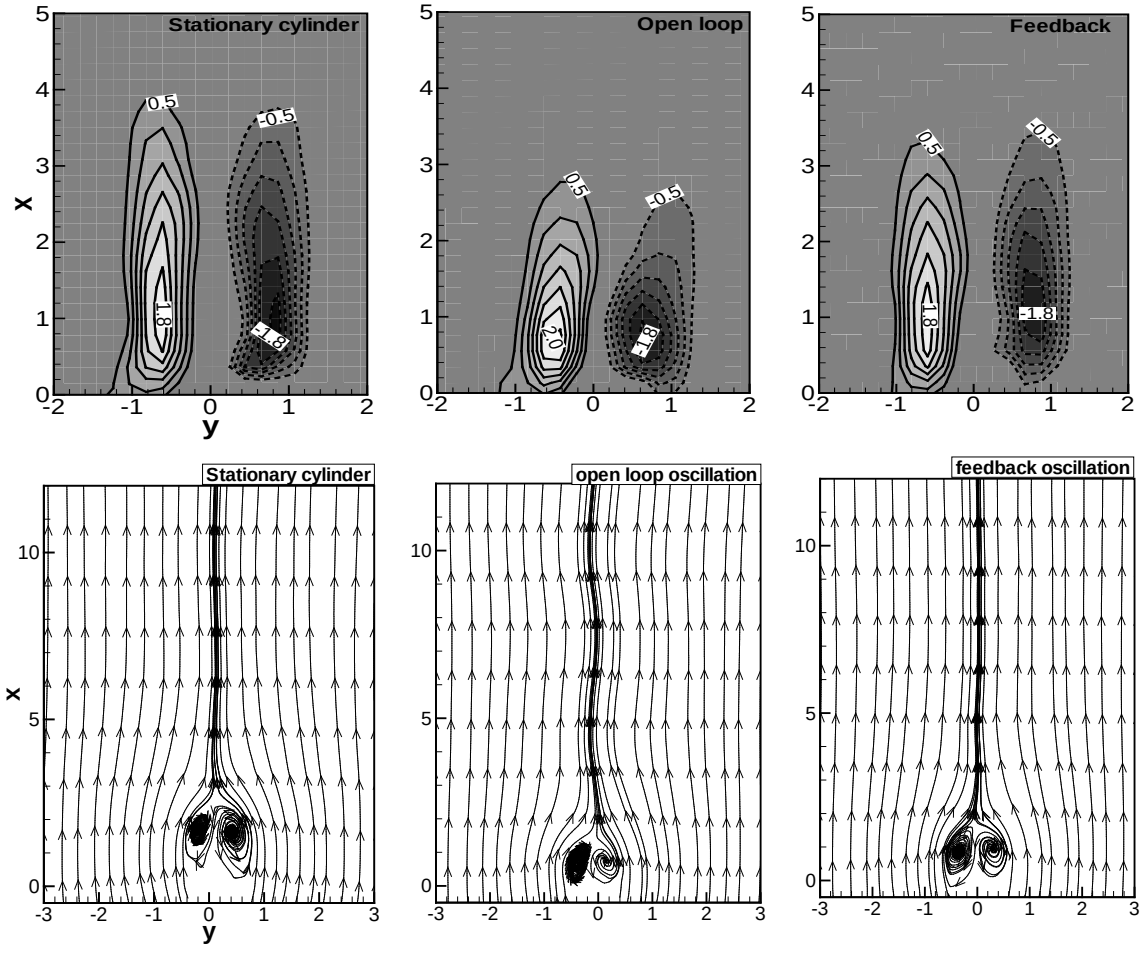

Figure 4 Time-averaged streamlines and vorticity contours in the wake of a stationary and an oscillating cylinder (with and without feedback) at Re=175.

concentration of vortices near the cylinder increases. The concentration of the maximum vorticity zone in the near field region confirms the reduction in the size of the recirculation zone, Figure 4(a). With feedback control, the concentration near the cylinder marginally decreases, indicating that feedback negates some of the beneficial aspects of forced oscillations. The vorticity production in the wake is proportional to the velocity difference between the main

stream and the cylinder centreline velocity. The time instant at which flow separation takes place on each side of the cylinder corresponds to distinct phases in the cylinder oscillation. Hence the vortices on either side of the cylinder are not necessarily of equal strength. The vorticity contours of Figure 4(b) show that, for the present experiments, the effect of oscillation on breaking flow symmetry is small. The influence on the time-averaged drag coefficient is, however, significant (Table 1).

D. Time-averaged Velocity and Velocity Fluctuations

Figure 5 shows the distributions of the time-averaged velocity components across the wake along with the velocity fluctuations. Velocity has been non-dimensionalized with that of the incoming stream and the spatial coordinates are non-dimensionalized by the cylinder edge. With an increase in downstream distance, the x-component of the centreline velocity recovers towards the free-stream value, while the y-component velocity approaches zero. Measurements at the streamwise location of x/B=4 are reported. The time-averaged velocity deficit is higher for the stationary cylinder when compared to the perturbed. The velocity deficit for the closed loop experiment is higher when compared to forced oscillations. The velocity deficit is a second measure of the time-averaged drag coefficient along with the wake size of the base region. Thus, for the present set of parameters, the control function (namely a phase shift of 180o) is seen to be ineffective in reducing the time-averaged drag coefficient beyond what is seen for forced oscillations. In contrast, it is shown later from instantaneous flow visualization images (Figure 9) that vortex shedding is weakened with feedback. The velocity signals of Figure 2 also show that the strength of the velocity fluctuations diminish in the presence of cylinder oscillations. The magnitudes of urms and vrms were measured to be nearly equal in experiments with and without feedback, but smaller than for the wake of a stationary cylinder.

Figure 6(a) shows the centreline recovery of streamwise velocity for stationary and oscillating cylinders, with and without feedback. The centreline velocity attains a minimum close to the cylinder and then increases as fluid is entrained from the region outside the wake. The minimum value attained close to the cylinder is a measure of the vortex strength in the base region. The centreline recovery directly relates to the wake width which in turn depends on entrainment at the edge of the wake. The average centreline velocity is lower inside the recirculation zone, where the transverse velocity is high. The recovery is faster in the near field region and reaches an asymptotic value at around x/B =7. The rate of velocity recovery is seen to be high for the open loop system when compared to the stationary and feedback control experiments. The weakening of the base region in terms of vorticity production is the greatest for the open loop oscillation when compared to feedback and stationary experiments. Reduction in drag coefficient seen in Table 1 is consistent with these trends.

Figure 6(b) shows the streamwise variation of the velocity fluctuations at the mid-plane of the cylinder. The objective of this plot is to demonstrate differences in the formation length of the vortices. For both experiments, stationary cylinder and with oscillation (open loop and feedback), the turbulence intensity increases in the streamwise direction, reaching a maximum value and is followed by slow decay. Higher turbulence intensities are realized for the oscillating cylinder (open loop and feedback) when compared to the stationary. Velocity fluctuations decay faster and reach an asymptotic value after a certain downstream distance. Figure 6(b) shows that feedback control was not able to attenuate velocity fluctuations below the value seen for a cylinder with forced oscillations.

Figure 7 shows the nondimensional contours of velocity fluctuations urms and vrms for the stationary and oscillating cylinder experiments. The turbulence intensity near the cylinder increases as more energy enters the flow field from the cylinder excitation. This effect, however, reduces when feedback control is applied to the cylinder oscillation. For open loop oscillation the flow field becomes asymmetric. The magnitude of fluctuations is also high near the cylinder for the open loop arrangement when compared to the experiment with feedback. With feedback control, the flow field becomes increasingly symmetric.

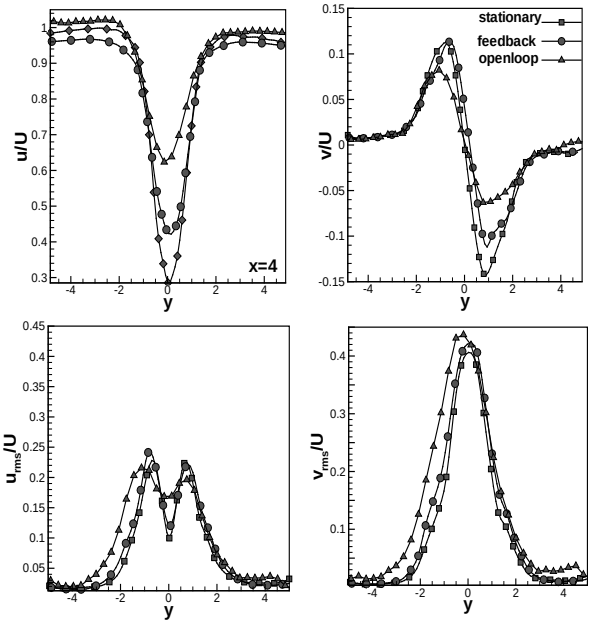

Figure 5 Comparison of time-averaged velocities u and v, velocityfluctuations urms and vrms for stationary and oscillating cylinders (with and without feedback) at a downstream location of x =4, Re=175.

E. Instantaneous Vorticity Field

Figure 8 shows the instantaneous contours of spanwise vorticity whose axis is parallel to that of the cylinder. Stationary and oscillating cylinders (with and without feedback) are shown at selected instants of time. Positive vorticity corresponds to clockwise rotation and is indicated by solid lines whereas the negative spanwise vorticity corresponds to counter clockwise rotation and is indicated by dashed lines. When there is no perturbation, the vortices display the pattern of a Karman vortex street. With forced perturbation, the vortices get distorted. The vortices are shed much closer to the cylinder and the longitudinal spacing of the vortices decreases. Time-wise periodicity is, however, preserved. These aspects

are discussed in the previous work of the authors (Dutta et al., 2007). With feedback control, the periodic structure is disrupted. Experiments show that the structure thus generated is not continuous and has intermittency.

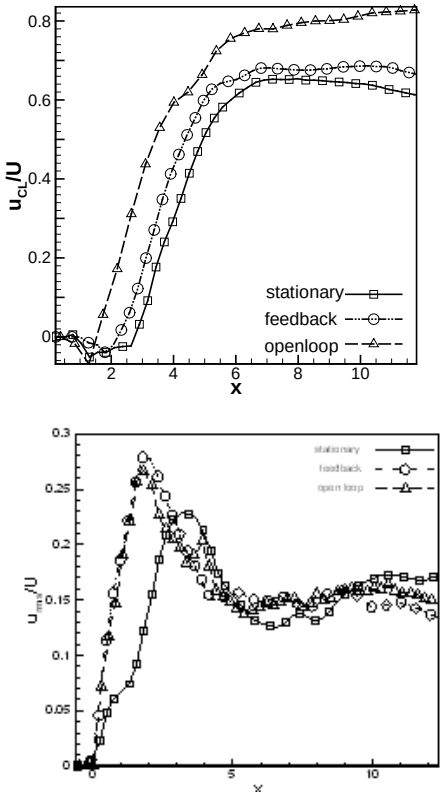

Figure 6 Centreline recovery of stream wise velocity and RMS fluctuations for stationary and oscillating cylinder (with and without feedback) at Re=175.

F. Flow Visualization Images

Figure 9 shows particle traces for stationary and the oscillation experiments for flow past a square cylinder. The top row shows a sequence of three instantaneous images for a stationary cylinder. The expected Karman vortex shedding pattern is to be seen in the images. The shedding mechanism is different for an oscillating cylinder when compared to the stationary. With oscillation at the vortex shedding frequency, the wake periodicity is governed by the amplitude of oscillation of the cylinder. Vortices are shed from points very near the cylinder. With the application of feedback to the actuator, vortex shedding is distorted and intermittently, the wake width considerably reduces. This pattern was not continuously seen with feedback. Vortex shedding such as that for a stationary cylinder was also seen, a trend seen in the velocity time traces of Figure 2.

G. Effect of Reynolds Number

Results discussed above are mainly at Reynolds number of 175. Experiments have also been carried out at Reynolds number of 355. Apart from the slight narrowing of the wake width, essentially, no difference was seen in the wake behaviour with an increase in Reynolds number. Figure 10 compares the images of particle traces in the wake when the cylinder is oscillated using feedback from the hotwire sensor. Intermittent reduction in the wake width is seen at both Reynolds numbers, though at different cylinder positions. At Re=355, vortex shedding is expected to show three dimensionality.

The time-averaged streamlines and vorticity plots are shown in Figure 11 for Re=175 and 355. The flow fields are similar in terms of symmetry, though the wake at Re=355 shows waviness in the streamline pattern and a slight displacement in the recirculation zone in the flow direction. These are expected trends for a higher Reynolds number. Figure 12 shows the comparison of percentage turbulence intensity for Reynolds number. Figure 12 shows the comparison of percentage turbulence intensity for feedback controlled oscillations at the two Reynolds numbers. The turbulence velocities are non-dimensionalized with the free stream velocity. The point of maximum turbulence intensity is located at the centre of the wake zone and is shown by a dark shade. The magnitudes of maximum turbulence intensity are quite close for both Reynolds numbers. While the time-averaged flow field shows a narrowing effect at higher Reynolds numbers, the turbulence field shows a slightly greater spread in the transverse direction. These trends match those seen in wakes of stationary cylinders as well as those subjected to forced oscillations.

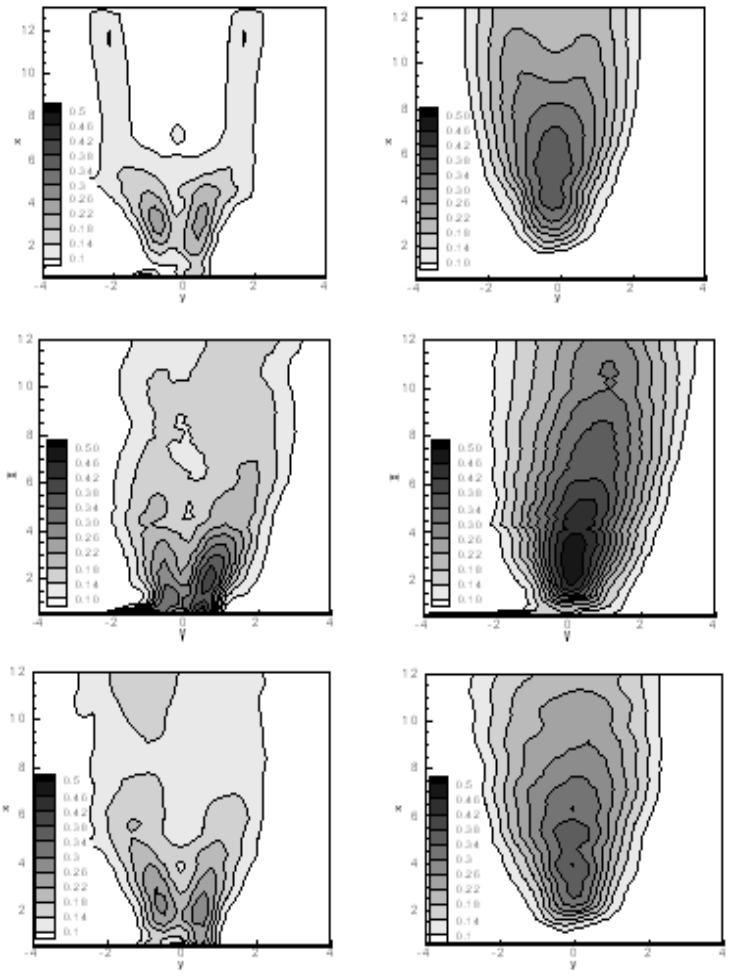

Figure 7 Nondimensional urms (left) and vrms (right) contours for stationary (top), open loop (middle) and closed loop (bottom) control.

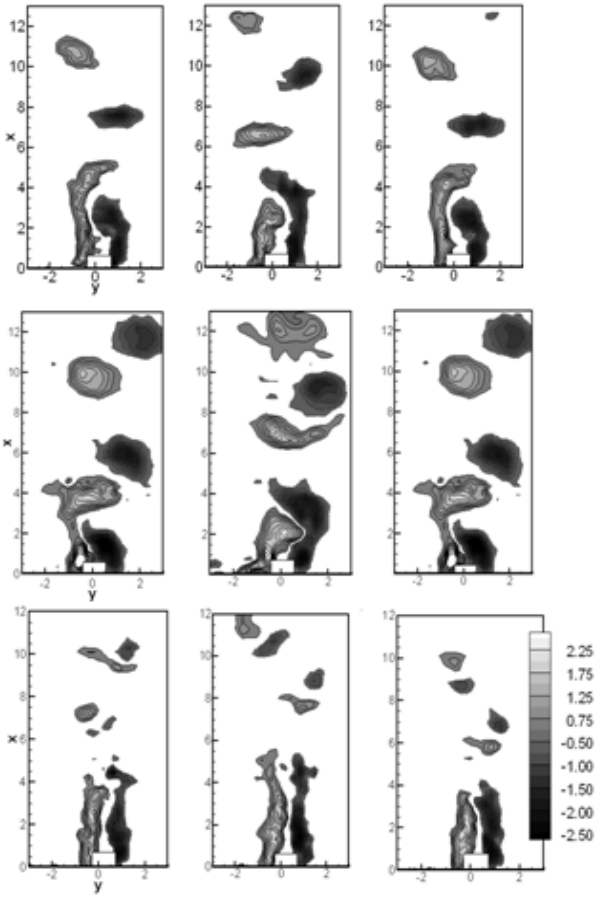

Figure 8 Instantaneous spanwise vorticity (ωz) contours for a stationary cylinder (top), oscillating cylinder without feedback (middle) and cylinder with feedback (bottom) cylinder at Re=175.

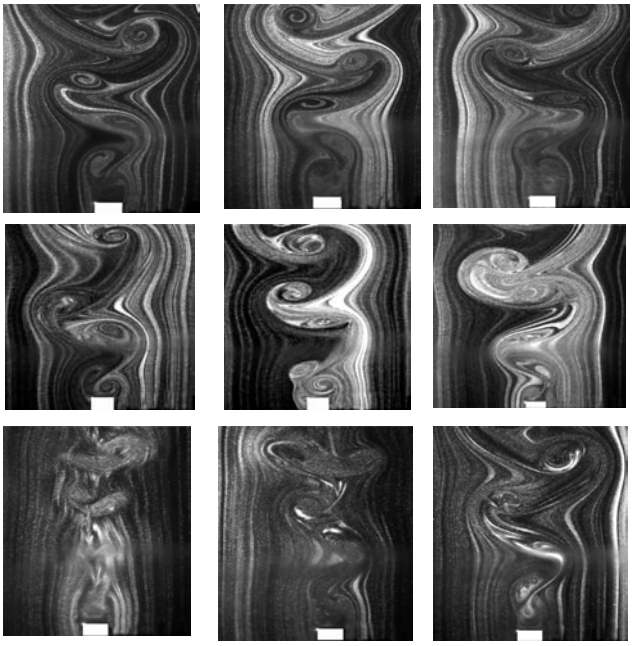

Figure 9 Instantaneous flow visualization images in the x-y plane for stationary (top row), open loop (middle) and closed loop oscillation (bottom row).

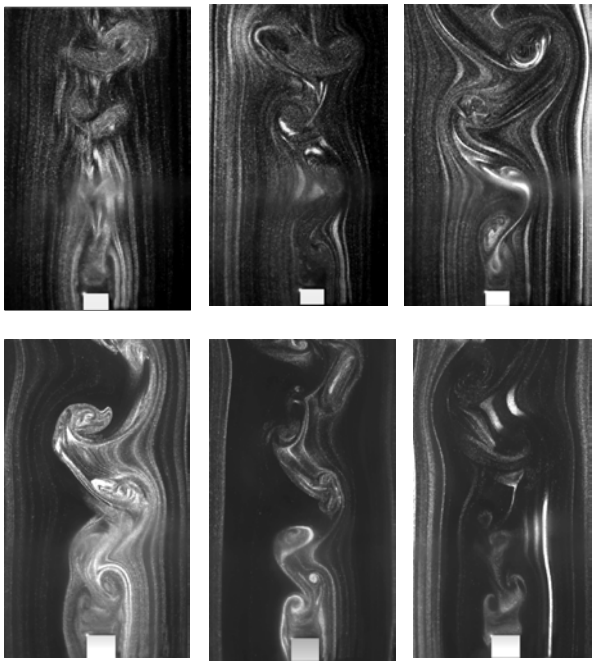

Figure 10 Instantaneous flow visualization images in the x-y plane for cylinder oscillation with feedback at Re=175 (top) and Re=355 (bottom).

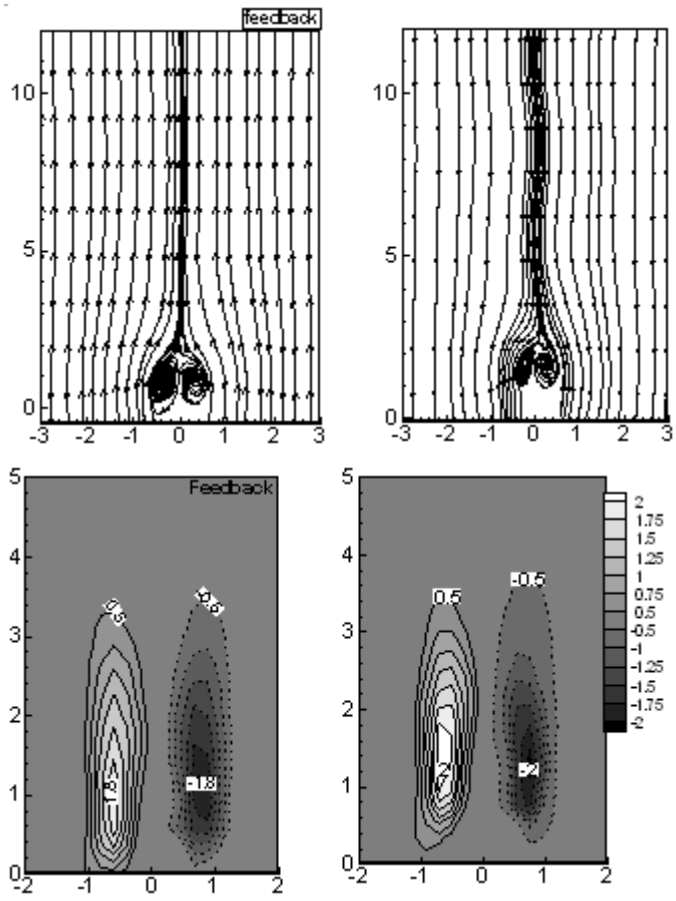

Figure 11 Streamlines and time-averaged spanwise vorticity contours (ωz) for cylinder oscillation with feedback. Re=175 (left) and Re=355 (right)

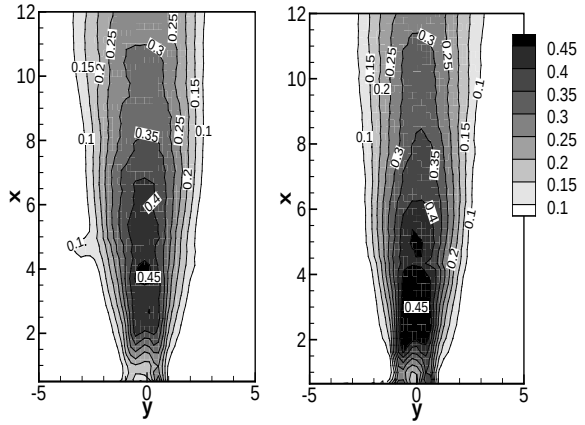

Figure 12 Contour plot of percentage turbulence intensity (u2rms +v2rms)0.5/U for cylinder oscillation with feedback. Re=175 (left) and Re=355 (right)

V. CONCLUSIONS

The flow field in the wake of a cylinder oscillated using feedback control was investigated in terms of instantaneous as well as time-averaged data. In the feedback mode, the cylinder was provided 180o phase-shifted signal with respect to the velocity signal in the near wake. Results were obtained primarily for a Reynolds number of 175. The instantaneous flow field showed intermittent suppression of vortex shedding and aperiodicity. Velocity fluctuations were a maximum for a stationary cylinder with lowest values for the cylinder oscillated at a fixed frequency, equal to the vortex shedding frequency of a stationary cylinder. The time-averaged flow field showed a smaller recirculation region both with open loop and feedback when compared to a stationary cylinder. The reduction in the wake size was greater for open loop control. The extent of symmetry in the time-averaged field was higher for the wake with feedback. Correspondingly, the time-averaged drag coefficient of a cylinder with forced oscillations was found to be 8% lower than the stationary cylinder, while, with feedback, the reduction was 5%. These results were generally realized at a Reynolds number of 355 as well. It is, thus, to be seen that the present scheme of feedback oscillation in not as beneficial as forced oscillations without feedback.

REFERENCES

[1] Choi, H., Jeon, W.P., and Kim, J., 2008, "Control of flow over a bluff body," Ann. Rev. Fluid Mech., 40, 113-139.

[2] Dutta, S, Panigrahi, P.K., and Muralidhar, K., 2008, "Experimental investigation of flow past a square cylinder at an angle of incidence," ASCE, J. Engg. Mechanics, 134, 788-803.

[3] Dutta, S. Panigrahi, P. K., and Muralidhar, K., 2007, "Sensitivity of a square cylinder wake to forced oscillations," ASME, J. Fluids Engg, 29, 852-870.

[4] Lu, B. and Bragg, M, B, 2002, "Experimental investigation of the wake survey method for a bluff body with a highly turbulent wake", paper number AIAA 2002-3060, presented at the 20th AIAA Applied Aerodynamics Conference, Missouri, USA.

[5] Pastoor, M., Henning, L., Noack, B. R. and Tadmor, G., 2008, "Feedback shear layer control for bluff body drag reduction," J. Fluid Mechanics, 608, 161-196.

[6] Zhang, M. M., Zhou, Y. and Cheng L., 2004, "Closed-loop-controlled vortex shedding and vibration of a flexibly supported square cylinder under different schemes," Phys. Fluids, 16 (5), 1439-1448.

[7] Zhang, M. M., Zhou, Y. and Cheng, L., 2003, "Spring Supported Cylinder Wake Control," AIAA Journal, 41, 1500-1506.

[8] Zhang, M. M., Zhou, Y. and Cheng L., 2005, "Closed-Loop-Manipulated Wake of a Stationary Square Cylinder," Expt. Fluids, 39, 75-85.

[9] Roussopoulos K.B. , 1993, "Feedback control of vortex shedding at low Reynolds numbers," J. Fluid Mech. , 248, 267-296.

[10] Warui, H.M.,and Fujisawa, N., 1996, " Feedback control of vortex shedding from a circular cylinder by cross-flow cylinder oscillations", Expt. Fluids, 21, 49-56.

[11] Huang, X.Y., 1996, " Feedback control of vortex shedding from a circular cylinder,"Expt. Fluids, 20, 218-224.

[12] Beaudoin, J.F., Cadot, O., Aider, J.L., Wesfried, J.E., 2006, " Drag reduction of a bluff body using adaptive control methods" Phys.fluids, 18, 085107.

[13] Tao, J.S., Huang, X.Y. and Chen W.K. , 1996" A flow visualization study of feedback control of vortex shedding from a circular cylinder, J. Fluid Mech. , 10, 965-970.